

Dynamics of an $SO(5)$ -symmetric ladder model

R. Eder¹, A. Dorneich¹, M. G. Zacher^{1,2}, W. Hanke¹, Shou-Cheng Zhang³

¹*Institut für Theoretische Physik, Universität Würzburg, Am Hubland, 97074 Würzburg, Germany*

²*Institut for Solid State Physics, University of Tokyo, Tokyo, Japan*

³*Department of Physics, Stanford University, Stanford, USA*

(December 3, 2017)

We discuss properties of a recently proposed exactly $SO(5)$ -symmetric ladder model. In the strong coupling limit we demonstrate how the $SO(3)$ -symmetric description of spin ladders in terms of bond Bosons can be upgraded to an $SO(5)$ -symmetric bond-Boson model, which provides a particularly simple example for the concept of $SO(5)$ symmetry. Based on this representation we show that antiferromagnetism on one hand and superconductivity on the other hand can be understood as condensation of either magnetic or charged Bosons into an RVB vacuum. We identify exact eigenstates of a finite cluster with general multiplets of the $SO(5)$ group, and present numerical results for the single particle, spin and charge spectra of the $SO(5)$ -symmetric model and identify ‘fingerprints’ of $SO(5)$ symmetry in these. In particular we show that $SO(5)$ symmetry implies a ‘generalized rigid band behavior’ of the photoemission spectrum, i.e. spectra for the doped case are rigorously identical to spectra for spin-polarized states at half-filling.

I. INTRODUCTION

It has recently been proposed [1] that the antiferromagnetic (AF) and superconducting (SC) phases of the high- T_c cuprates are unified by an $SO(5)$ symmetry principle. A remarkable degree of continuity between insulating and doped phase is indeed supported by a considerable body of numerical evidence [2–5]. Further support for this proposal came from numerical investigations, which demonstrated that the low-energy excitations of physical models for the high- T_c materials, i.e. $t-J$ and Hubbard models, can be classified in terms of an $SO(5)$ -symmetry multiplet structure [6,7]. In these two-dimensional (2D) microscopic models, the undoped situation - in agreement with the experimental situation in the cuprates - corresponds to that of a Mott insulator with broken $SO(3)$ or spin rotational symmetry: long-range AF order is realized. The $SO(5)$ -symmetry principle then tells us how this long-range magnetic order and the accompanying low-energy spin excitations are mapped onto the corresponding off-diagonal long-range SC order and the low-energy “Goldstone bosons” (the π -mode) in the doped situation [8,6,7].

However, there exists also a second class of Mott-type insulators without long-range AF order, i.e. spin liquids, which have a gap to spin excitations. There is growing experimental evidence that they are also intimately related to the physics of high- T_c compounds: not only do these compounds show above the Neél temperature and superconducting transition temperature at small dopings signs of such a spin gap, but there exist also copper-oxides with a CuO_2 plane containing line-defects, which result in ladder-like arrangements of Cu -atoms [9–12]. These systems can be described in terms of coupled two-leg ladders [12], which exhibit a spin gap in the insulating compound and thus belong to the spin-liquid Mott-insulator variety. Also the related “stripe phases” of the 2D CuO_2

planes in the cuprate superconductors have recently received considerable attention [13,14]. In these systems, the apparent connection between the spin gap and superconductivity must be explained.

In order to illustrate how the $SO(5)$ theory can, in principle, cope with this challenge, an exactly $SO(5)$ invariant ladder model has recently been constructed [15]. It was shown that a 2-leg ladder with entirely local interactions, i.e. an on-site interaction $|U| \gg t$, where t denotes the chain hopping, an intra-rung interaction $|V| \gg t$ and a magnetic rung-exchange interaction J can have $SO(5)$ symmetry if these interactions are related to each other in a specific way, i.e. $J = 4(U+V)$. The ground-state phase diagram of this model was determined in strong coupling and, in particular, a regime identified, where the strong-coupling ground state is a spin-gap insulator. In addition, the spin-gap magnon mode of the Mott insulator was shown to evolve continuously into the π -resonance mode of the superconductor.

However, two key questions remained open, the first being the relationship of this $SO(5)$ ladder to the “physical” $t-J$ or Hubbard ladders and the second regarding the connection to the other variety of Mott insulators, i.e. the ones with long-range AF order.

With regard to the first question, progress was recently made in the regime of weak-coupling: using the weak-coupling renormalization group method, two independent works [16,17] have recently demonstrated that rather generic ladder models at half-filling flows to an $SO(5)$ symmetric fixed point.

In the present work, we try to attack both questions in the experimentally relevant intermediate and strong-coupling regimes. The basic idea is to derive the $SO(5)$ concept for a ladder or, more generally, for a spin liquid with an “RVB vacuum” instead of an “Neél vacuum” involving a physically appealing new construction: an effective $SO(5)$ invariant low-energy Hamiltonian is con-

structured in terms of a bond operator representation. In strong coupling, this is a well-established concept for spin ladders [18,19] to account quantitatively for the spin excitations of Heisenberg ladders (up to the physically most relevant case of isotropic couplings in the rungs and along the ladder). The spin excitations are described in terms of triplet fluctuations around the RVB vacuum. The new idea is to combine this $SO(3)$ -symmetric description of the spin degrees of freedom, i.e. the triplet excitations, with the charge (hole) dynamics. This is accomplished by introducing two new Bosons on a rung which stand for charge fluctuations, i.e. empty and fourfold occupied rungs. When combined into a 5-dimensional Boson-vector, the dynamics of spin and charge excitations is captured by a manifestly $SO(5)$ invariant Hamiltonian. It is shown that this formulation in terms of triplet and hole fluctuations around an “RVB vacuum” allows for a physically transparent demonstration of the corner stone in $SO(5)$ theory, i.e. that AF and SC are “two faces of one and the same coin”. By starting from this “RVB vacuum”, which represents the spin liquid state at half-filling, we demonstrate that an AF ordered state can be generated by forming a coherent state

$$|\psi\rangle \sim e^{\lambda t_z^\dagger(q=\pi)} |\Omega\rangle,$$

which corresponds to z -like triplets condensed into the $q = \pi$ state. However, in the $SO(5)$ theory, the z -like triplet with momentum π and the hole pair with momentum 0 are components of one and the same $SO(5)$ vector. They are rotated into each other by the $SO(5)$ generating operator π . This implies that the above coherent state with condensed triplets can be $SO(5)$ -rotated into a corresponding coherent state with $t_z^\dagger(q = \pi)$ replaced by the (hole-) pair creation operator $\Delta^\dagger(q = 0)$. This state corresponds to hole pairs condensed into the $q = 0$ state, i.e. a superconducting state. In other words: both the AF and the SC state can be viewed as a kind of condensation out of the RVB state, or the spin liquid. If the so constructed AF state is the actual ground state at half-filling, then this physically very appealing $SO(5)$ construction yields automatically the ground state in the doped situation, i.e. the SC state.

This construction can also shed light on the second of the above questions, namely the interrelation between the spin gap Mott-insulator and superconductivity. The construction presented here rests on the special geometry of the 2-leg ladder, which suggests a unique “RVB vacuum”, from which the AF coherent state can be obtained. In $2 - D$, such a unique vacuum does, in general, not exist, unless one takes the growing experimental evidence for some form of spatial inhomogenities such as stripes [13,14] into account. However, even for a translationally invariant state, up to an additional statistical average over all possible dimer (singlet) coverings of the plane, the analogue of the triplet-like exci-

tation in the ladder can still be generated: here singlet-dimers are substituted by triplet-dimers and this excited dimer propagates through the $2D$ -system. Again, the $SO(5)$ π -operator converts excited dimers with momentum (π, π) into $d_{x^2-y^2}$ -symmetry hole pairs with momentum $(0, 0)$. A description of spin excitations in $2D$ in terms of Boson-like excited dimers, as for the ladder considered here, may thus be a natural starting point for clarifying the role of the spin gap (for which the ladder is a “toy model”) and thus the role of the spin-liquid Mott-insulators for superconductivity, in general. This will be discussed in a forthcoming paper [26].

The first question, i.e. the adiabatic connection between the $SO(5)$ symmetric model and “physical” ladder models, such as the $t - J$ model, is answered numerically in the present work. This is achieved by a kind of “Landau mapping” of the single- and two-particle excitations of the $SO(5)$ ladder model onto the corresponding excitations of the $t - J$ ladder.

As mentioned above, the empty-fourfold rung fluctuation involves, in principle, a high energy (of order $\simeq 2U$). In the $SO(5)$ description, the Hamiltonian is supplemented by a term which contains density and exchange interactions, and which physically pulls down the empty-fourfold fluctuation to be degenerate with the triplet-triplet fluctuation. It has been shown in Ref. [15] that this can be achieved already for purely local interactions V and J within the rungs by choosing $4(U + V) = J$. We demonstrate numerically that, and give physical reasons why, this at first sight rather unphysical parameter condition nevertheless gives in fact an astonishingly good mapping of the $SO(5)$ model onto the $t - J$ model for the low-energy ω versus momentum q dynamics. These findings strongly support the physical relevance of the $SO(5)$ description in physical ladder models, such as Hubbard and $t - J$ models, which are of the spin-liquid Mott insulator variety.

The paper is organized as follows: Sec. II describes the construction of an $SO(5)$ symmetric ladder model in terms of bond-triplet and -charge bosons, which are unified into a common $SO(5)$ vector $(\vec{t})_i$. It also contains the coherent-state description, where an AF ordered state with staggered magnetization in z -direction is generated by a condensation of z -like triplet excitations. When the triplets are rotated (via the π -operator) onto the corresponding hole pairs (with $d_{x^2-y^2}$ symmetry), a $d - SC$ state results. Sec. III then contains a general representation of the $SO(5)$ multiplet structure in terms of irreducible representations in the $Q - S_z$ plane (here $Q = (N_e - N)/2$ with N_e the number of electrons and N the number of sites [1] is the pair density and S_z the z -component of total spin). We consider here the previously studied multiplets of diamond shape [7] (corresponding to even numbers of electrons or holes, i.e. electron or hole pairs) as well as multiplets evolving to

a square shape. The latter correspond to odd numbers of charge carriers and are thus required for building up selection rules for photoemission. Sec. IV verifies these selection rules in exact diagonalizations of 2×6 $SO(5)$ ladders. Similarly, sec. V numerically illustrates the spin and charge dynamics of the exact $SO(5)$ model and checks corresponding selection rules for spin- and charge correlation functions. Sec. VI discusses the ‘‘Landau mapping’’ and adiabatic connection to the physical $t - J$ model, and sec. VII gives a short conclusion.

II. ELEMENTARY EXCITATIONS OF THE LADDER

We begin with the standard Hubbard model on a 2-leg ladder, i.e.

$$H = - \sum_{i,j} t_{ij} c_{i,\sigma}^\dagger c_{j,\sigma} + U \sum_i (n_{i,\uparrow} - \frac{1}{2})(n_{i,\downarrow} - \frac{1}{2}). \quad (1)$$

The nearest-neighbor hopping integral along the legs will be called t , the one within the rungs t_\perp , and U denotes the on-site Coulomb repulsion. We assume the strong coupling limit, $U/t, U/t_\perp \gg 1$ and start out with the case of half-filling and vanishing leg-hopping t . The system then decomposes into an array of Heitler-London type dimers and the ground state is simply the product of singlets along the rungs of the ladder, with energy $E_G \approx -2Nt_\perp^2/U$, where $N/2$ is the number of rungs.

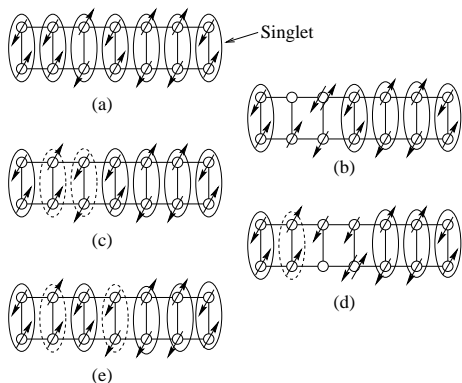


FIG. 1. Starting from the RVB vacuum (a) the ‘virtual’ hopping process (a) \rightarrow (b) \rightarrow (c) leads to the pair creation of two triplets (indicated by dashed lines). Further virtual hopping processes such as (c) \rightarrow (d) \rightarrow (e) enable the propagation of the triplets along the ladder

This state is frequently referred to as the ‘rung RVB state’ and has been the basis of many theoretical works on spin ladders [18–20]. Next, let us consider the effect of switching on t . This will produce charge fluctuations, and hence exchange processes along the legs. These lead, as a first step, to the ‘pair creation’ of triplets along the legs. In subsequent steps, these newly created triplets

can propagate along the ladder (see Figure 1). Introducing operators which create singlets and triplets [21]:

$$\begin{aligned} s_{ij}^\dagger &= \frac{1}{\sqrt{2}}(\hat{c}_{i,\uparrow}^\dagger \hat{c}_{j,\downarrow}^\dagger - \hat{c}_{i,\downarrow}^\dagger \hat{c}_{j,\uparrow}^\dagger), \\ t_{ij,x}^\dagger &= -\frac{1}{\sqrt{2}}(\hat{c}_{i,\uparrow}^\dagger \hat{c}_{j,\uparrow}^\dagger - \hat{c}_{i,\downarrow}^\dagger \hat{c}_{j,\downarrow}^\dagger), \\ t_{ij,y}^\dagger &= \frac{i}{\sqrt{2}}(\hat{c}_{i,\uparrow}^\dagger \hat{c}_{j,\uparrow}^\dagger + \hat{c}_{i,\downarrow}^\dagger \hat{c}_{j,\downarrow}^\dagger), \\ t_{ij,z}^\dagger &= \frac{1}{\sqrt{2}}(\hat{c}_{i,\uparrow}^\dagger \hat{c}_{j,\downarrow}^\dagger + \hat{c}_{i,\downarrow}^\dagger \hat{c}_{j,\uparrow}^\dagger), \end{aligned} \quad (2)$$

we can write the rung-RVB state (which we henceforth consider as a kind of ‘vacuum’), as

$$|\Omega\rangle = \prod_{n=1}^{N/2} s_n^\dagger |0\rangle. \quad (3)$$

Here, the site indices along a rung, (i, j) , have been replaced by a single index n labelling the rung. It has been shown by Gopalan *et al.* [18] that the dynamics of the triplets can be mapped *exactly* onto a system of three species of hard-core bond-Bosons on a 1D chain. Thereby the presence of the Boson t_a^\dagger on some site means that the corresponding rung is in the triplet a state - absence of any Boson implies that the rung is in the singlet state. The 3 components of the triplet on the n^{th} rung form a 3-dimensional vector

$$\boldsymbol{\tau}_n^\dagger = \begin{pmatrix} t_{n,x}^\dagger \\ t_{n,y}^\dagger \\ t_{n,z}^\dagger \end{pmatrix} \quad (4)$$

and the Hamiltonian operator governing the triplet-like Bosons can be cast into the following manifestly $SO(3)$ invariant form [18,19]:

$$\begin{aligned} H &= J_\perp \sum_n \boldsymbol{\tau}_n^\dagger \cdot \boldsymbol{\tau}_n \\ &+ \frac{J}{2} \sum_n (\boldsymbol{\tau}_n^\dagger \cdot \boldsymbol{\tau}_{n+1}^\dagger + H.c.) + \frac{J}{2} \sum_n (\boldsymbol{\tau}_n^\dagger \cdot \boldsymbol{\tau}_{n+1} + H.c.) \\ &- \frac{J}{2} \sum_n : (\boldsymbol{\tau}_n^\dagger \cdot \boldsymbol{\tau}_{n+1}^\dagger \boldsymbol{\tau}_{n+1} \cdot \boldsymbol{\tau}_n \\ &\quad - \boldsymbol{\tau}_n^\dagger \cdot \boldsymbol{\tau}_{n+1} \boldsymbol{\tau}_{n+1}^\dagger \cdot \boldsymbol{\tau}_n) : \end{aligned} \quad (5)$$

Here $::$ as usually denotes normal ordering and the parameters are $J=4t^2/U$ and $J_\perp=4t_\perp^2/U$. The terms in (5) describe the ‘energy of formation’ of a triplet (1st term); the pair creation of two triplets on neighboring rungs (2nd term); the propagation of a triplet (3rd term), the simultaneous ‘species flop’ of two triplets on neighboring rungs (4th term); and the exchange of two triplets (5th term) [18,19].

Let us now consider a new type of fluctuation. Once a charge fluctuation has been created one might envisage

that the remaining electron in the singly occupied rung follows suit, so that the resulting state has one empty rung, and a fourfold occupied rung (see Figure 2). Again,

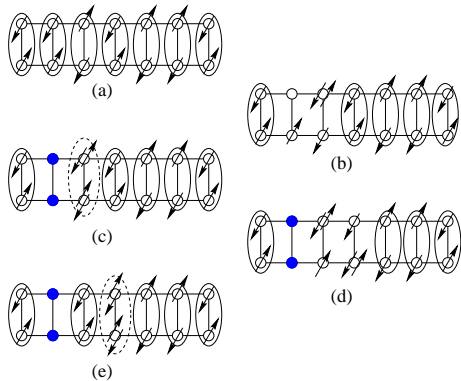


FIG. 2. A second type of fluctuation which leads to the creation of charged rungs: starting from the vacuum, (a) \rightarrow (b) \rightarrow (c) leads to the creation of an empty and a fourfold occupied rung. Further virtual hopping processes such as (c) \rightarrow (d) \rightarrow (e) enable the propagation of these charged excitations.

in subsequent steps the empty and fourfold occupied rung can propagate, in much the same way as the triplets did. Clearly, the fourfold occupied rung has a very high energy $\approx 2U$. Following Ref. [15] however, we now amend the Hamiltonian with the goal to ‘pull down’ this state in energy, so as to make the empty-fourfold state degenerate with the triplet-triplet state. This can be achieved by adding terms of the form

$$H_1 = \sum_{i,j} V_{i,j} (n_i - 1)(n_j - 1) + \sum_{i,j} J_{i,j} \mathbf{S}_i \cdot \mathbf{S}_j, \quad (6)$$

where $n_i = \sum_{\sigma} c_{i,\sigma}^{\dagger} c_{i,\sigma}$ is the operator of electron density on site i , and \mathbf{S}_i the operator of electron spin. It has been shown in Ref. [15] that by retaining only a density interaction V and exchange constant J within the rungs, and choosing $U + V = J/4$, one can reach a situation where the empty-fourfold fluctuation in Figure 2c is precisely degenerate with the triplet-triplet fluctuation in Figure 1c, and both of them are lower than the singly-threefold intermediate state (Figure 1b, Figure 2b). In the following, we call the energy of the singlet E_0 , that of the triplet/empty/fourfold occupied rung E_1 and that of a singly/threefold occupied rung E_2 . The situation we want to reach is $E_0 < E_1 \ll E_2$. We would like to stress that the parameters we need to choose to reach this ($U + V = J/4$) are rather unphysical. Physically, if we want J and U to be positive and J not to be too large, this requires a large negative rung interaction V . However, for the time being we ignore this complication and defer a discussion of the case $H_1 \rightarrow 0$ to the end of this section.

If we restrict the Hilbert space to only rung triplets and singlets, the Hamiltonian (5) remains valid also for the

$SO(5)$ symmetric ladder. The only difference is a change of J to $J' = 4t^2/(E_2 - E_1)$ and a change of the Boson’s ‘energy of formation’ from $J_{\perp} \rightarrow \Delta_1 = E_1 - E_0$. Our goal is now to simply retain this Hamiltonian, but enlarge the 3-dimensional vector $\boldsymbol{\tau}$ into a 5-dimensional vector comprising 2 additional Bosons which represent the empty and fourfold occupied rung. We introduce new Bosons h and d , whose presence on a rung implies that the rung is empty or fourfold occupied:

$$\begin{aligned} h_{i,j}^{\dagger} &\rightarrow |vac\rangle \\ d_{i,j}^{\dagger} &\rightarrow -c_{j,\uparrow}^{\dagger} c_{i,\uparrow}^{\dagger} c_{j,\downarrow}^{\dagger} c_{i,\downarrow}^{\dagger} |vac\rangle \end{aligned} \quad (7)$$

(the extra minus sign makes sure that the state corresponding to $d_{i,j}^{\dagger}$ can be written as $\Delta_{i,j}^{\dagger} s_{i,j}^{\dagger}$, with Δ the singlet-pairing operator along a rung). Just as two singlets on neighboring rungs can convert themselves in a kind of pair creation process (Figure 1a \rightarrow Figure 1c) into two triplets, they can also convert themselves into an empty rung and a fourfold occupied rung. And, similarly as a triplet can exchange itself with a singlet, so can an empty or doubly occupied rung. An analogous process to the 4th term would be the conversion of two triplets on neighboring rungs into an empty and a fourfold occupied rung. And finally, an empty rung can exchange itself also with a triplet, which corresponds to the 5th term. in Eqn.(5).

The empty rungs and fourfold occupied rungs thus will act ‘almost’ like the triplets - there is, however, a subtle and crucial difference. Careful calculation shows that all matrix elements for pair creation and propagation of the empty and fourfold occupied rungs have the same magnitude, but *opposite sign* as for the triplet rungs. The ultimate reason is that a spin-flip (which propagates a triplet) is accomplished by a back-and-forth motion of electrons, and hence picks up a Fermi minus sign, whereas the propagation of an empty rung corresponds to a net movement of charge in one direction, and hence gets no Fermion minus sign. We cope with this by a rung-dependent gauge transformation for the charged Bosons and introduce:

$$\begin{aligned} t_{n,1}^{\dagger} &= e^{i\pi n} \frac{1}{\sqrt{2}} (d_n^{\dagger} + h_n^{\dagger}), \\ t_{n,5}^{\dagger} &= e^{i\pi n} \frac{i}{\sqrt{2}} (d_n^{\dagger} - h_n^{\dagger}). \end{aligned} \quad (8)$$

The extra phasefactor $e^{i\pi n}$ precisely cancels the minus sign in the matrix elements of the two new Bosons, so that we can now describe the physics of the Bosons by the following manifestly $SO(5)$ invariant Hamiltonian

$$\begin{aligned} H &= \Delta_1 \sum_n \mathbf{t}_n^{\dagger} \cdot \mathbf{t}_n \\ &+ \frac{J'}{2} \sum_n (\mathbf{t}_n^{\dagger} \cdot \mathbf{t}_{n+1}^{\dagger} + H.c.) + \frac{J'}{2} \sum_n (\mathbf{t}_n^{\dagger} \cdot \mathbf{t}_{n+1} + H.c.) \end{aligned}$$

$$- \frac{J'}{2} \sum_n : (\mathbf{t}_n^\dagger \cdot \mathbf{t}_{n+1}^\dagger \mathbf{t}_{n+1} \cdot \mathbf{t}_n - \mathbf{t}_n^\dagger \cdot \mathbf{t}_{n+1} \mathbf{t}_{n+1}^\dagger \cdot \mathbf{t}_n) : \quad (9)$$

Here \mathbf{t} denotes the 5-dimensional vector

$$\mathbf{t}_n^\dagger = \begin{pmatrix} t_{n,1}^\dagger \\ t_{n,x}^\dagger \\ t_{n,y}^\dagger \\ t_{n,z}^\dagger \\ t_{n,5}^\dagger \end{pmatrix}. \quad (10)$$

In terms of this 5-dimensional Boson-vector on a single rung the 10 root generators of $SO(5)$ take the simple form (suppressing the rung index)

$$L_{ab} = -i(t_a^\dagger t_b - t_b^\dagger t_a), \quad (11)$$

which for $x \leq a, b \leq z$ reduces to a representation of the $SO(3)$ spin operators in the rung basis [19]. Bearing in mind that the \mathbf{t} are hard-core Bosons, it is straightforward to show that the operators (11) obey the $SO(5)$ angular momentum algebra [1]:

$$[L_{ab}, L_{cd}] = -i(\delta_{ad}L_{bc} - \delta_{ac}L_{bd} + \delta_{bc}L_{ad} - \delta_{bd}L_{ac}). \quad (12)$$

Choosing $\alpha \in x, y, z$, the combination

$$\pi_\alpha = \frac{1}{\sqrt{2}}(L_{1\alpha} - iL_{\alpha 5}) \quad (13)$$

replaces an a -type triplet with momentum $k = \pi$ by a hole pair along the rungs with momentum $k = 0$ - this operator is therefore nothing but the ladder equivalent of the π -operator in 2D [1], which replaces a triplet with momentum (π, π) by a $d_{x^2-y^2}$ hole pair with momentum $(0, 0)$.

We can also express the $SO(5)$ hard-core Boson Hamiltonian (9) directly in terms of a $SO(5)$ quantum nonlinear σ model Hamiltonian by introducing the $SO(5)$ super-spin vector at a given rung as

$$x_a = \frac{1}{\sqrt{2}}(t_a + t_a^\dagger) \quad (14)$$

and its conjugate momentum as

$$p_a = \frac{1}{i\sqrt{2}}(t_a - t_a^\dagger). \quad (15)$$

In this representation, the symmetry generator takes the more familiar form

$$L_{ab} = x_a p_b - x_b p_a \quad (16)$$

Using these operator identities, the $SO(5)$ hard-core Boson Hamiltonian (9) can be expressed as (repeated $SO(5)$ indices are summed over!)

$$H = \frac{\Delta_1}{4} \sum_n L_{ab}^2(n) + J' \sum_n x_a(n)x_a(n+1) + \frac{J'}{4} \sum_n L_{ab}(n)L_{ab}(n+1) \quad (17)$$

This Hamiltonian is quantized using the $SO(5)$ commutation relations (12) and

$$[L_{ab}, x_c] = -i(\delta_{bc}x_a - \delta_{ac}x_b), \quad (18)$$

together with the hard core constraint

$$x_a x_b = \delta_{ab}. \quad (19)$$

The $SO(5)$ ladder model can be used for a particularly simple and transparent demonstration of the key feature of the $SO(5)$ theory, namely the one-to-one correspondence of antiferromagnetism and superconductivity. The ground state of the ladder models is actually an RVB type of vacuum without AF long-range-order. However, for illustrative purposes, let us now construct an AF ordered state (which is in general not an eigenstate of the Hamiltonian) by condensing the magnons into the RVB ground state. We can obviously express the operator of staggered magnetization in z -direction as

$$M_s = \sum_n e^{i\pi n} (P_n(\uparrow\downarrow) - P_n(\downarrow\uparrow)),$$

where e.g. $P_n(\uparrow\downarrow)$ projects onto states where the n^{th} rung has the configuration $\uparrow\downarrow$. It is now easy to see that

$$\begin{aligned} (P_n(\uparrow\downarrow) - P_n(\downarrow\uparrow)) s_n^\dagger &= t_{n,z}^\dagger, \\ (P_n(\uparrow\downarrow) - P_n(\downarrow\uparrow)) t_{n,a}^\dagger &= \delta_{a,z} s_n^\dagger, \end{aligned} \quad (20)$$

whence

$$M_s = \sqrt{\frac{N}{2}} [t_z^\dagger(q = \pi) + t_z(q = \pi)].$$

If we now form the coherent state

$$|\Psi_\lambda\rangle = \frac{1}{\sqrt{n}} e^{\lambda\sqrt{N}t_z^\dagger(q=\pi)} |\Omega\rangle,$$

which corresponds to z -like triplets condensed into the $k=\pi$ state, and treat the \mathbf{t} as ordinary Bosons, we obtain

$$\langle \Psi_\lambda | M_s | \Psi_\lambda \rangle = \sqrt{2}\lambda N.$$

If the hard-core constraint is taken into account rigorously, the only change is an extra correction factor of $1/(1 + \lambda^2)$ on the r.h.s., see the Appendix.

This calculation shows that by starting from an ‘RVB vacuum’, an antiferromagnetically ordered state with M_S in z -direction can be generated by condensing z -like triplet-excitations into the $k=\pi$ state. At this point we can invoke the $SO(5)$ symmetry of the model, which tells us that since the z -like triplet with momentum π and the

hole pair with momentum 0 are two different components of a 5-vector (the difference in momenta is precisely absorbed by the gauge transformation (8) we needed to make the signs of hopping integrals consistent), they are dynamically indistinguishable. This means that the AF state, with condensed triplets, can be $SO(5)$ -rotated into a state with condensed hole pairs. It follows that if the antiferromagnetic state were the ground state at half-filling (which is the case for 2D materials) we can replace all z -like triplets by hole pairs with momentum 0 and by $SO(5)$ symmetry automatically obtain the ground state in the doped case. The latter then consists of hole-pairs along the rungs condensed into the $k = 0$ states and thus is necessarily superconducting. In other words: both the antiferromagnetic and the superconducting state may be viewed as some kind of condensate ‘on top of’ the rung-RVB state. $SO(5)$ symmetry then simply implies that the condensed objects are combined into a single vector, whence the unification of antiferromagnetism and superconductivity follows in a most natural way.

The above derivation makes sense only in a strong coupling limit, where a discussion starting out from rung-singlets makes sense. One might expect, however, that similar considerations will apply also for cases with a weak coupling within the rungs [16,17].

To conclude this section, we discuss what will happen if we switch off the correction terms (6), which were introduced so as to enforce exact $SO(5)$ symmetry. The crucial question is whether above considerations will retain some validity or break down altogether. Let us consider the 1 – 5 plane of the 5-dimensional space, i.e. the ‘charge-like subspace’. In the fully $SO(5)$ -symmetric model the vector \mathbf{t} can be rotated freely in this plane. The total charge is related to the angular momentum in the 1 – 5 plane, since $Q = L_{15} = x_1 p_5 - x_5 p_1$. For a system with a large charge gap compared with the spin gap, one can apply a chemical potential to lower the energy of the empty rungs $h_n^\dagger|0\rangle$ at the cost of further increasing the energy of the fourfold occupied rungs $d_n^\dagger|0\rangle$. The chemical potential acts like a magnetic field normal to the 1 – 5 plane, and selects a particular sense of the rotation in the 1 – 5 plane. Therefore, the “free rotor” in the exact $SO(5)$ symmetric models becomes a “chiral rotor” in the more realistic Hubbard or $t - J$ models.

In terms of the Boson model, switching off H_1 will lead to different energies for the different Boson species, i.e. a replacement of the form

$$\Delta_1 \sum_n \mathbf{t}_n^\dagger \cdot \mathbf{t}_n \rightarrow \sum_n \epsilon_0 h_n^\dagger h_n + J \boldsymbol{\tau}_n^\dagger \cdot \boldsymbol{\tau}_n + \epsilon_2 d_n^\dagger d_n,$$

where ϵ_0 corresponds to the binding energy of a hole pair (relative to the rung singlet) and $\epsilon_2 \approx 2U$. Here we are neglecting the modification of the off-diagonal matrix elements $\propto J'$. While ϵ_2 is a huge energy, let us assume that we have a state with $Q \leq 0$ and treat this term in perturbation theory. The crucial point is now, that for

total electron density ≤ 1 the fourfold occupied rung d_n^\dagger is admixed only as a quantum fluctuation, so that we expect for the change in energy

$$\delta E = (\epsilon_0 - \Delta_1)Q + 0\left(\left(\frac{J'}{E_1 - E_0}\right)^2\right).$$

In the limit $J' \ll E_1 - E_0$ the main effect of switching to the physical Hubbard or $t - J$ model *in the hole-doped subspace* thus is adding a chemical potential-like term $(\epsilon_0 - \Delta_1)Q$ to the Hamiltonian. Apart from that, having $\epsilon_2 \rightarrow 2U$ for states with $Q \leq 0$ merely corresponds to projecting out quantum fluctuations involving charged Bosons. This may be expected to have only a minor effect. Of course states with $Q > 1$ will have their energies shifted by $Q\epsilon_2$, so that $SO(5)$ rotations into this sector of the Hilbert space become forbidden. As long as we restrict ourselves to hole-doped states, however, one may hope that $SO(5)$ symmetry remains approximately valid. Below we will present an explicit numerical check of this more qualitative discussion.

III. CLASSIFICATION OF STATES ACCORDING TO $SO(5)$ MULTIPLETS

In this section we shall briefly review the $SO(5)$ group theory and classify all states in the ladder model according to irreducible representations (irreps) of the $SO(5)$ Lie algebra. We also discuss various $SO(5)$ selection rules which shall be used in the next two sections.

In reference [7], three of us showed how low lying bosonic states in the $t - J$ model can be classified by the fully symmetric tensor multiplets of the $SO(5)$ Lie algebra. The full multiplet structure of the $SO(5)$ group is much richer. The general irreps of an $SO(5)$ -symmetric model are described by two integers

$$(p, q), p \geq q \geq 0 \quad (21)$$

with dimension

$$D = (1 + q)(1 + p - q) \left(1 + \frac{1}{2}p\right) \left(1 + \frac{1}{3}(p + q)\right), \quad (22)$$

and Casimir [22]

$$C = \frac{1}{2}p^2 + \frac{1}{2}q^2 + q + 2p. \quad (23)$$

$SO(5)$ is a rank two algebra so we choose the charge Q and the z -component of the Spin S_z as members of the Cartan subalgebra of mutually commuting generators. This allows us to draw the different irreps in the $Q - S_z$ plane. The (p, p) irreps have the familiar [7] diamond shape and corresponds to the fully symmetric traceless

tensor irreps identified in [7]. The $(p, 0)$ irreps form a square in the $Q - S_z$ plane and are the spinor states found in systems with odd number of electrons. For example, the quintet E_1 manifold with 3 magnons and 2 pair states carry the label $(1, 1)$, while the quartet E_2 manifold with one or three electrons per rung carries the label $(1, 0)$. The intermediate multiplets $(p, p > q > 0)$ are the evolution from the square to the diamond (Figure 3). All states of the exact $SO(5)$ symmetric models

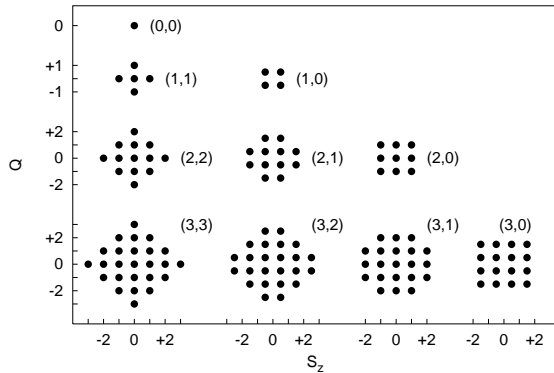


FIG. 3. The first few irreps of $SO(5)$ displayed on the $Q - S_z$ -plane. The (p, p) multiplets have the familiar diamond shape; with $(p, q < p)$ the multiplets evolve to a square shape. The number of dots in each multiplet is not the full dimension of the $SO(5)$ -irrep since there are additional degeneracies in the S_z -direction.

constructed in [15] can be classified into this $SO(5)$ multiplet structure. We have verified this numerically by computing the energies and expectation values of the Casimir operator for *all* eigenstates of a 2×4 system. By scanning all sectors of different hole number and z -spin and collecting states of equal (within computer accuracy, i.e. 10^{-12}) energy and Casimir charge we have verified that from the ground states up to the highest excited states all eigenstates of the system can be classified into the multiplets shown in Figure 3 (and more complicated ones). For the 2×6 system, where a full diagonalization is not feasible anymore, we have verified this for the low energy states obtainable by Lanczos diagonalization. Besides classifying eigenstates into $SO(5)$ multiplet structures, $SO(5)$ symmetry also gives powerful selection rules on the possible transition processes and relates various matrix elements through the Wigner-Eckart theorem. In the following two sections, we are interested in the photoemission, charge and spin spectra of the $SO(5)$ symmetric ladder model. The perturbing operator in the photoemission process is a single electron operator, which transforms according to the 4 dimensional $(1, 0)$ irreps under $SO(5)$. In this work, we shall consider the initial and final states of the form (p, p) , corresponding to excited magnon and pair states. The possible final states generated by the perturbing operator can be obtained by decomposing the product representation into irreducible

components, and it given by

$$(1, 0) \otimes (p, p) = (p + 1, p) + (p, p - 1) \quad (24)$$

Similarly, the perturbing operator in the neutron scattering or Josephson tunneling process transform according to the 5 dimensional $(1, 1)$ irreps under $SO(5)$. The possible final states are given by the following decomposition rules:

$$(1, 1) \otimes (p, p) = (p + 1, p + 1) + (p + 1, p - 1) + (p - 1, p - 1) \quad (25)$$

The photoemission selection rules (except for $S \rightarrow S \pm \frac{1}{2}$) can be easily visualized by superimposing the involved $SO(5)$ -multiplets (Figures 4 and 5). Figure 4 shows that there are four possible photoemission and inverse photoemission transitions for the $S_z = 0$ state at half-filling which belongs to the $(1, 1)$ multiplet. We

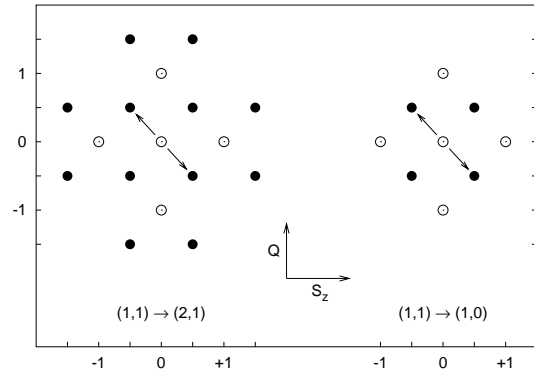


FIG. 4. Visualization of the selection rules for photoemission and inverse photoemission for $SO(5)$ symmetric states on the example of a transition originating from a half filled state with $S_z = 0$ in the $(1, 1)$ multiplet. $SO(5)$ selection rules only allow transitions to the $(1, 0)$ and the $(2, 1)$ multiplets (black discs), which are superimposed on the initial $(1, 1)$ multiplet (circles). In this example, the photoemission and inverse photoemission process remove/inject a spindown-electron so the photoemission transition is visualized by an arrow pointing south-east and the inverse photoemission arrow points towards north-west.

therefore expect four distinct bands in the spectrum. If, on the other hand, one takes a spin-polarized or doped state of the same multiplet as the initial state for photoemission and inverse photoemission we expect to see only three bands since there are only three possible transitions according to the selection rules (Figure 5). Furthermore, we expect the *very same* spectrum for both the polarized and the doped case since the initial states belong to the same initial multiplet as well as all target states belong to the same target multiplets and are therefore degenerate.

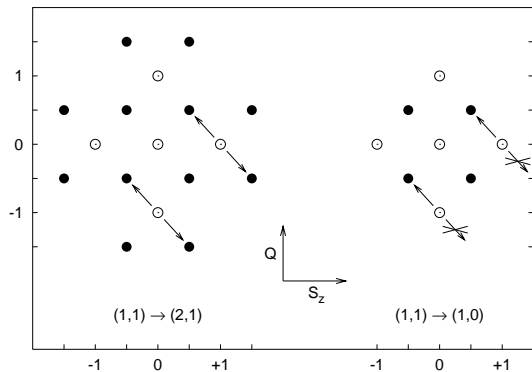


FIG. 5. Photoemission and inverse photoemission originating from a spin-polarized half-filled state ($Q = 0, S_z = +1$) and from a doped state ($Q = -1, S_z = 0$). Both states are members of the $(1, 1)$ multiplet like the initial state in Figure 4. This Figure shows that there is no allowed photoemission transition to the $(1, 0)$ multiplet for either of the two states.

IV. SINGLE PARTICLE SPECTRA

We now want to see the practical application of the selection rules discussed in the preceding section. To that end we study the photoemission (PES) and inverse photoemission (IPES) spectrum, which we define as

$$A_{PES}(\mathbf{k}, \omega) = \frac{1}{\pi} \Im \langle 0 | c_{\mathbf{k}\downarrow}^\dagger \frac{1}{\omega + H - \epsilon_0 - i0^+} c_{\mathbf{k}\downarrow} | 0 \rangle,$$

$$A_{IPES}(\mathbf{k}, \omega) = \frac{1}{\pi} \Im \langle 0 | c_{\mathbf{k}\downarrow} \frac{1}{\omega - H + \epsilon_0 - i0^+} c_{\mathbf{k}\downarrow}^\dagger | 0 \rangle.$$

Here $|0\rangle$ is a suitably chosen initial state and ϵ_0 its energy. In the following, we will label different states as ${}^m \mathbf{K}_Q$, where m denotes the standard spin multiplicity, \mathbf{K} the total momentum and Q the charge quantum number. For finite clusters of our $SO(5)$ symmetric ladder model this is readily obtained numerically by Lanczos diagonalization [23]. The $SO(5)$ multiplets discussed above are easily identified, because the energies of states belonging to one multiplet are degenerate (i.e. identical to computer accuracy). This allows to study the evolution of the single-particle spectral function as we pass from one multiplet (p, q) to the other, and within one multiplet through the different doping levels. To begin with, Figure 6 shows the single-particle spectrum for the half-filled ground state ${}^1(0, 0)_0$, which actually forms a one-dimensional $(0, 0)$ multiplet. Final states can only belong to the 4-dimensional $(1, 0)$ representation, see Figure 3. Despite the fact that we are using very strong interaction parameters, there is just one single electron-like band in PES, whose dispersion closely follows the noninteracting dispersion. The center of gravity of this band is given by the energy difference between a rung-singlet and a singly occupied rung, i.e. $E_0 - E_2 = -7U/2 - 3V$, i.e. -10 with our present parameter values. We proceed to the spectrum of the ${}^3(\pi, \pi)_0$ state, with $S_z=0$ - this state

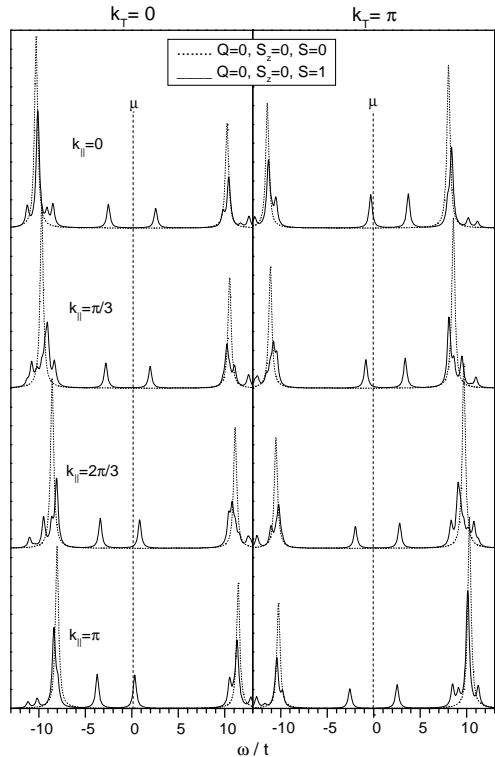


FIG. 6. Comparison of the single particle spectral function for the half-filled ground state (dotted line) and the half-filled ${}^3(\pi, \pi)_0$ state with $S_z=0$ (full line). The Fermi energy, defined as the average of first ionization and affinity energy, is taken as the zero of energy. The parameter values are $t = 1$, $t_\perp = 1$, $U = 8$, $V = -6$, and $J = 8$.

belongs to the fivefold degenerate ($p = 1, q = 1$) multiplet. From Figure 4 we expect final states belonging to both the $(2, 1)$ and the $(1, 0)$ representation. It appears as if the bands seen in the ground state spectra remain practically unchanged - as a new feature, however, there appear some weak ‘sidebands’ close to μ . They can be seen both in photoemission and in inverse photoemission, so that we obviously have precisely the 4 bands expected on the basis of our discussion of selection rules given above (see Figure 4). The physical interpretation is straightforward. The ${}^3(\pi, \pi)_0$ state has a single triplet-like Boson. The ‘main bands’, which are similar to those in the ground state spectra, correspond to final states where the photohole is generated in a singlet-rung. They therefore contain the original triplet, plus a singly occupied rung which propagates through the ladder and carries the entire momentum transfer. These states therefore belong to the $(2, 1)$ representation. The center of gravity of this band is again at $E_0 - E_2$. The two excitations (triplet and hole) now can scatter from each other, whence the respective band becomes broadened. There is however

also a second process, namely the photohole can be created in the rung occupied by the triplet. This creates final states containing only a singly occupied rung, which must therefore belong to the $(1,0)$ representation. As the intensity of this second process is proportional to the triplet density, our interpretation of the sidebands can be checked numerically by comparing the mean weight of the sidebands for one-triplet-states on ladders with different numbers of rungs. On 4-, 6-, and 8-rung ladders (which corresponds to triplet densities of $1/4$, $1/6$, and $1/8$) and with our parameter values, we found mean weights of 0.276, 0.183, and 0.137 – a convincing proof of the interpretation given above. The center of gravity

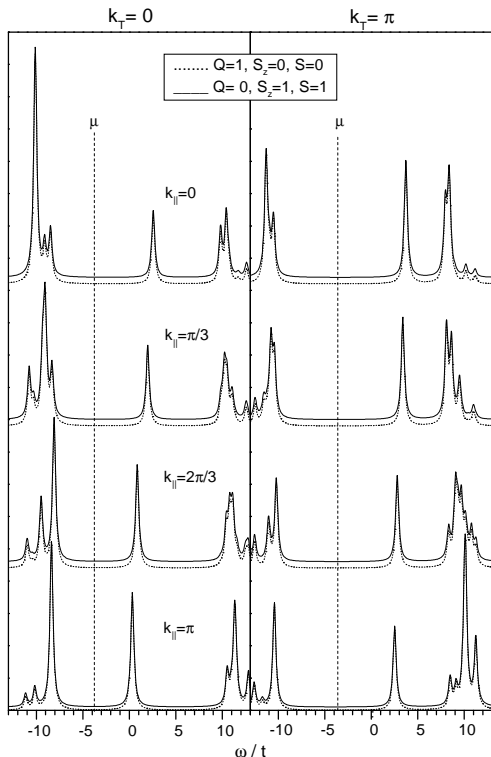


FIG. 7. Comparison of the electron removal spectrum for the two-hole ground state $^0(0,0)_{-1}$ (dotted line) and the half-filled $^3(\pi,\pi)_0$ state with $S_z=1$ (full line). The removed electron has \downarrow -spin. The spectra for the half-filled state have been offset in y -direction so as to facilitate the comparison. Parameter values are as in Figure 6.

of the resulting band is at the energy difference between a rung triplet and a singly occupied rung, $E_1 - E_2 = U/2 + V$, i.e. -2 with our parameters. In this type of process the photohole has to absorb also the momentum of the triplet, (π, π) , so that the *dispersion* of this band is precisely the same as that of the ‘main band’ seen for the $^1(0,0)_0$ ground state, but shifted by (π, π) (note however the rigid shift of the band by $E_1 - E_0$ due to the difference in initial state energy). Literally the same arguments hold for the inverse photoemission part, and

inspection of Figure 6 shows that all of these features are observed.

So far we have seen that spin excitations in the ground state generate additional sidebands in the single particle spectrum. At this point, however, we can invoke the exact $SO(5)$ symmetry of the model, which tells us that spin polarization and hole/electron doping are equivalent, in that the empty rung is the ‘ $SO(5)$ partner’ of the triplet rung. Consequently, Figure 7 compares the single particle spectrum of the $^1(0,0)_{-1}$ and $^3(\pi,\pi)_0$ states. Both states belong to the same $(1,1)$ representation – unambiguous evidence is provided by the fact that their energies agree to computer accuracy. In Figure 7 we have chosen the $S_z=1$ member of the triplet, and study the annihilation of a \downarrow -electron. From Figure 5 we expect that this simulation probes exclusively the $(2,1)$ representation. Since the final states for these two different processes belong to the same $SO(5)$ multiplet, we expect their amplitudes to be directly related. More precisely we have $|^3(\pi,\pi)_0\rangle = \pi_+^\dagger |^1(0,0)_{-1}\rangle$, with $\pi_+^\dagger = \pi_x^\dagger + i\pi_y^\dagger$, whence:

$$\begin{aligned} & \langle ^3(\pi,\pi)_0, S_z = 1 | c_{\mathbf{k}\downarrow}^\dagger \frac{1}{\omega + H - \epsilon_0} c_{\mathbf{k}\downarrow} | ^3(\pi,\pi)_0, S_z = 1 \rangle \\ &= \langle ^1(0,0)_{-1} | \pi_+ c_{\mathbf{k}\downarrow}^\dagger \frac{1}{\omega + H - \epsilon_0} c_{\mathbf{k}\downarrow} \pi_+^\dagger | ^1(0,0)_{-1} \rangle \\ &= \langle ^1(0,0)_{-1} | c_{\mathbf{k}\downarrow}^\dagger \frac{1}{\omega + H - \epsilon_0} [\pi_+, \pi_+^\dagger] c_{\mathbf{k}\downarrow} | ^1(0,0)_{-1} \rangle, \\ &= \langle ^1(0,0)_{-1} | c_{\mathbf{k}\downarrow}^\dagger \frac{1}{\omega + H - \epsilon_0} c_{\mathbf{k}\downarrow} | ^1(0,0)_{-1} \rangle, \end{aligned}$$

Where we have used the fact that the π_+ operator commutes with $c_{\mathbf{k}\downarrow}$ and the Hamiltonian. Furthermore, it annihilates the $|^1(0,0)_{-1}\rangle$ state. Since they belong to the same $SO(5)$ multiplet, the energies of the $|^1(\pi,\pi)_0\rangle$ and the $|^0(0,0)_{-1}\rangle$ state are identical, i.e. ϵ_0 . Therefore, as we indeed see in Figure 7, these two correlation functions are completely identical (within computer accuracy in the simulation). The physical reason is that the photohole cannot be created in the triplet rung (because the latter contains two \uparrow -electrons). In other words, when ‘seen through the eyes of the photohole-operator’ the triplet rung looks like it were ‘empty’, i.e. occupied by holes. *SO(5) symmetry thus implies that the single particle spectra in the doped ground states actually are identical to those of certain states at half-filling.* $SO(5)$ thus presents a very obvious rationalization for the rigid-band behavior observed numerically in the single particle spectra of the 2D $t - J$ model [2,5].

Next, we return to the photoemission spectrum for the $S_z=0$ member of the $^3(\pi,\pi)_0$ state. In this case, the photohole can be generated in the triplet rung, and, as discussed above, the sidebands near μ appear. The corresponding final states have only one singly occupied rung remaining in the system. Then, precisely the same kind

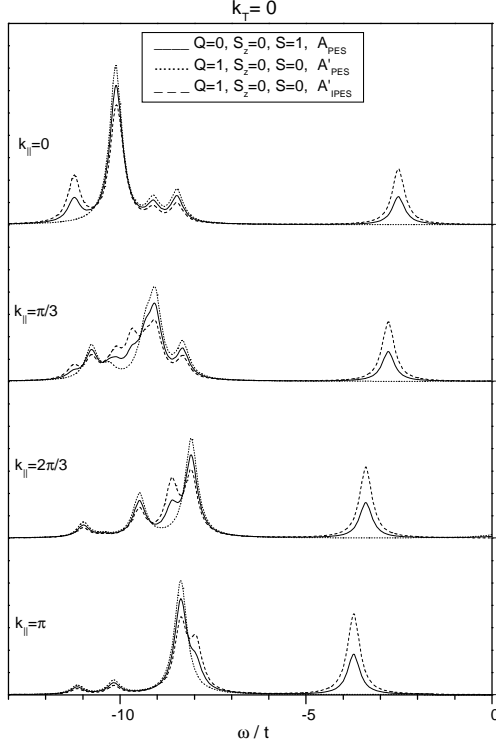


FIG. 8. Comparison of the electron removal spectrum for the two-hole ground state $A'_{PES}(\mathbf{k}, \omega)$ (dotted line), the ‘inverted’ electron addition spectrum for the two-hole ground state $A'_{IPES}(-\mathbf{k} + \mathbf{Q}, -\omega)$ (dashed line) and the electron removal spectrum $A_{PES}(\mathbf{k}, \omega)$ for the ${}^3(\pi, \pi)_0$ state with $S_z=0$ (full line). Parameter values are as in Figure 6.

of state results if a photoelectron is *created* in an empty rung. The only difference is, that in the former case the photohole has to absorb the momentum of the triplet i.e. (π, π) . We can conclude that the sideband seen in PES at half-filling must disappear in PES for the two-hole case, but reappear in IPES, shifted by (π, π) . This can also be seen explicitly by the following identity:

$$\begin{aligned}
& \langle {}^3(\pi, \pi)_0, S_z = 0 | c_{\mathbf{k}\downarrow}^\dagger \frac{1}{\omega + H - \epsilon_0} c_{\mathbf{k}\downarrow} | {}^3(\pi, \pi)_0, S_z = 0 \rangle \\
&= \langle {}^1(0, 0)_{-1} | \pi_z c_{\mathbf{k}\downarrow}^\dagger \frac{1}{\omega + H - \epsilon_0} c_{\mathbf{k}\downarrow} \pi_z | {}^1(0, 0)_{-1} \rangle \\
&= \frac{1}{2} \langle {}^1(0, 0)_{-1} | c_{\mathbf{k}\downarrow}^\dagger \frac{1}{\omega + H - \epsilon_0} c_{\mathbf{k}\downarrow} | {}^1(0, 0)_{-1} \rangle, \\
&+ \frac{1}{2} \langle {}^1(0, 0)_{-1} | c_{-\mathbf{k}+\mathbf{Q}\uparrow} \frac{1}{\omega + H - \epsilon_0} c_{-\mathbf{k}+\mathbf{Q}\uparrow}^\dagger | {}^1(0, 0)_{-1} \rangle,
\end{aligned}$$

where the second term in the last equation arises from the nonvanishing commutator between π_z and $c_{\mathbf{k}\downarrow}$. This identity implies that

$$A_{PES}(\mathbf{k}, \omega) = \frac{1}{2} [A'_{PES}(\mathbf{k}, \omega) + A'_{IPES}(-\mathbf{k} + \mathbf{Q}, -\omega)]. \quad (26)$$

Remarkably enough, the photoemission spectrum A_{PES} of the half-filled triplet $S_z = 0$ state is related to the photoemission spectrum A'_{PES} and inverse photoemission spectrum A'_{IPES} of the two hole ground state. Inspection of Figure 8 shows the three spectra in question demonstrates that the photoemission spectrum for the doped ground state (full line) indeed is simply the *mean* of the two spectra computed for the doped case.

All in all, the preceding discussion has shown that $SO(5)$ symmetry leads to at first sight unexpected behavior in the single-particle spectral function: since spin-polarization and hole doping are equivalent under $SO(5)$, the PES spectra of half-filled but spin-polarized states are identical to those of doped states. This may be the key to understand the rigid-band behavior observed [2,5] in the 2D $t - J$ model. Moreover, sidebands which appear in PES on spin-excited states at half-filling and which originate from processes where a spin excitation is annihilated, reappear in IPES on hole-doped states. Again, this was found previously also for the 2D $t - J$ model [24]. We note that the spectroscopies shown in Figures 6, 7, and 8 have been performed for the actual 2D $t - J$ model as well and have produced results in strong support of $SO(5)$ [26].

V. SPIN AND CHARGE DYNAMICS

Our rung-Boson model gives a description of the physics in terms of spinful and charged 2-electron excitations, and thus should be directly applicable to a discussion of the spin and charge dynamics. We introduce the spin correlation function (SCF) and the density correlation function (DCF) as

$$D_s(\mathbf{k}, \omega) = \frac{1}{\pi} \Im \langle 0 | S_{-\mathbf{k}}^z \frac{1}{\omega - H + \epsilon_0 - i0^+} S_{\mathbf{k}}^z | 0 \rangle,$$

$$D_c(\mathbf{k}, \omega) = \frac{1}{\pi} \Im \langle 0 | n_{-\mathbf{k}} \frac{1}{\omega - H + \epsilon_0 - i0^+} n_{\mathbf{k}} | 0 \rangle,$$

where S^z and n denote the operator of z -spin and electron density. As a first step we need representations of these operators in terms of the rung-Boson operators \mathbf{t} . Following Ref. [19], the spin operators for the n^{th} rung and the two possible momenta in y -direction are:

$$\mathbf{S}(n, 0) = \boldsymbol{\tau}_n^\dagger \times \boldsymbol{\tau}_n \quad (27)$$

$$\mathbf{S}(n, \pi) = \frac{1}{\sqrt{2}} (\boldsymbol{\tau}_n^\dagger + \boldsymbol{\tau}_n). \quad (28)$$

The spin operator with transverse momentum 0 thus actually corresponds to a two-particle spectrum, and thus will take (in an infinite system) the form of a continuum, whereas the spin operator with transverse momentum π

is a single particle-like spectrum. This difference can indeed be seen in the numerical spin correlation function (Ref. [19]).

The ‘ $SO(5)$ partner’ of the operator $\mathbf{S}(n, \pi)$ therefore is

$$\tilde{\Delta}_n = \frac{1}{\sqrt{2}}(t_{n,1}^\dagger + t_{n,1}), \quad (29)$$

which is related to the creation and annihilation of a singlet electron pair. On the other hand, the operator of electron density with transverse momentum 0 is the ‘ $SO(5)$ partner’ of $\mathbf{S}(k, 0)$:

$$n_{n,0} = i(t_{n,1}^\dagger t_{n,5} - t_{n,5}^\dagger t_{n,1}), \quad (30)$$

where $t_{n,1}^\dagger$ and $t_{n,5}^\dagger$ were defined in (8). Comparing (30), (27) to (11) we note that the density and spin operators for transverse momentum transfer 0 are actually root generators of $SO(5)$ - it follows that we can invoke the Wigner-Eckart-theorem (or intuitive arguments) to show that the respective spin and density spectra for certain pairs of states are identical. Below we will present various examples.

As for the density operator with transverse momentum transfer π , this is much more complicated because this operator annihilates any state corresponding to either charged or spinful Bosons. This correlation function therefore will be determined by the dynamics of the singly and threefold occupied rung, which in our strong coupling limit is admixed only virtually. We therefore expect that this correlation function has only weak features at relatively high energies.

After these preliminaries we proceed to a discussion of the numerical spectra. With regards to the SCF it is important to keep in mind that all following spectra have been computed using the z -component of the spin operator.

The half-filled ground state does not contain any Bosonic excitation at all. We can obtain a nonvanishing SCF only by coupling to the weakly admixed singly and threefold occupied rung, and therefore expect an extremely weak signal for $k_T=0$. Final states for the SCF with $k_T=\pi$ are in the $(1,0)$ representation, and the dominant peak in the respective spectra therefore gives the dispersion of the triplet Boson (see Figure 9). Choosing now the lowest of these $(1,1)$ states, the ${}^3(\pi, \pi)_0$, as the initial state for the calculation of the SCF with $k_T=0$, the triplet Boson with momentum $k=\pi$ could in principle be scattered into a state with momentum $k + \pi$, where k is the momentum transfer along the ladder. Since we are using the S_z operator, however, this is not possible (see the representation (27)) if we use the $S_z=0$ member of the ${}^3(\pi, \pi)_0$ state. We therefore expect a very low intensity spectrum which again is due to virtually admixed singly and three-fold occupied rungs. Moreover, since the z -like triplet acts precisely like a hole pair, and since the hole

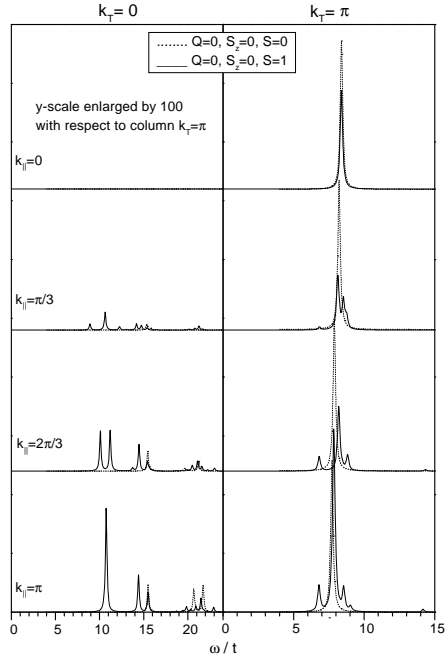


FIG. 9. Comparison of the spin correlation spectrum for the half-filled ground state (dotted line) and the ${}^3(\pi, \pi)_0$ state with $S_z=0$ (full line). Parameter values are as in Figure 6.

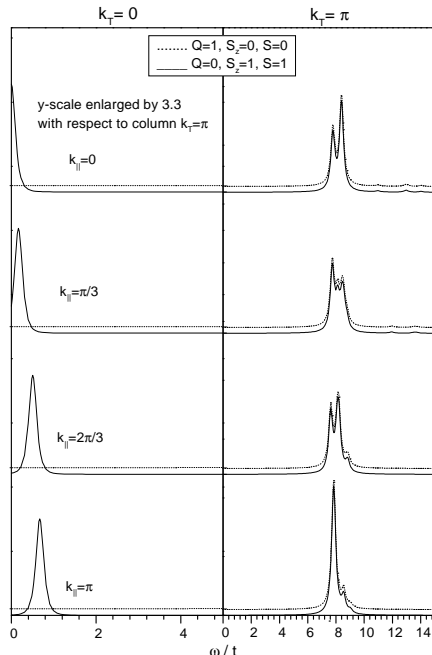


FIG. 10. Comparison of the spin correlation spectrum for the two-hole ground state (dotted line) and the half-filled ${}^3(\pi, \pi)_0$ state with $S_z=1$ (full line). The spectra for the two-hole state have been offset in y -direction to facilitate the comparison. Parameter values are as in Figure 6.

pair cannot be excited by the spin operator either, the $k_T=0$ spectra of the ${}^3(\pi, \pi)_0$ state with $S_z=0$ and the ${}^1(0, 0)_{-1}$ ground state must be identical by $SO(5)$ symmetry (which indeed they are, compare Figure 11). The situation changes completely if we use the $S_z=1$ member of the ${}^3(\pi, \pi)_0$ triplet as initial state (see Figure 10): this state contains a mixture of the x -like and y -like triplet, which both can be excited by the S_z -operator with $k_T=0$. We will therefore see a strong peak, with essentially the same dispersion as the dominant peak in the $k_T=\pi$ spectra in Figure 9, but shifted by $\Delta k=\pi$ in momentum and by $\approx E_1 - E_0$ in energy. On the other hand acting with the z -like spin operator with $k_T=\pi$ creates or annihilates a z -like Boson. Then, in both states, ${}^3(\pi, \pi)_0$ with $S_z=1$ and ${}^1(0, 0)_{-1}$, annihilation of a z -like Boson is not possible. Creating a z -like Boson, we will generate $SO(5)$ equivalent states, because the created z -like Boson interacts with the one already present in the system (x -like, y -like or hole-like) in identical ways - the $k_T=\pi$ spectra for these states thus must be identical, which indeed they are (compare Figure 10). Comparing Figure 10 with Figure 9 we see that the magnon mode with (π, π) at half-filling evolves continuously into the π resonance mode of the two hole state, in accordance with the analysis of reference [15]. Away from (π, π) , a lower energy structure emerges in the SCF of the two hole state.

On the other hand, when we switch to ${}^3(\pi, \pi)_0$ with $S_z=0$, the parts corresponding to a creation of the z -like Boson are slightly different from the spectra in Figure 10 because the final state now contains two Bosons of equal (z -like) species, which interact differently as compared to unequal species.

We proceed to a discussion of the DCF. In the remainder of this section we will refer only to spectra with $k_T=0$. It follows by $SO(5)$ symmetry and (27), (30) that the density operator with $k_T=0$ takes a completely analogous form as the spin operator. When using an $SO(5)$ singlet as initial state, both operators thus must give the same spectrum. This can be seen by comparing the SCF and DCF for the half-filled ground state, compare Figure 9 and 12. They are also identical when acting onto states which contain only z -like Bosons - which can be excited neither by the S_z or the density operator. This explains the identity of the SCF and DCF for the ${}^3(\pi, \pi)$ state with $S_z=0$, compare Figure 9 and Figure 12.

On the other hand, since the hole pair behaves like a triplet, the DCF for the two-hole ground state must be identical to the SCF for the ${}^3(\pi, \pi)_0$ state with $S_z=1$, compare Figures 10 and 12, right panel.

Summarizing this section, we have seen that $SO(5)$ symmetry enforces identity relationships between spin and charge correlation functions for different initial states, which differ by their hole number. Again this implies strong continuity with hole doping. While such continuity is certain to be present in any system with (approximate) $SO(5)$ symmetry, it should be noted that the

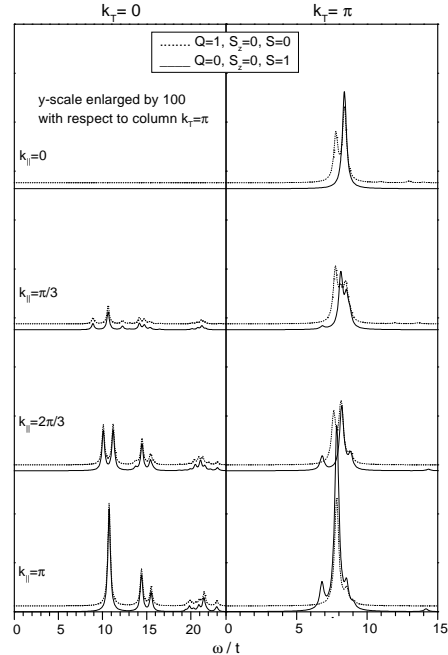


FIG. 11. Comparison of the spin correlation spectrum for the two-hole ground state (dotted line) and the ${}^3(\pi, \pi)_0$ state with $S_z=0$ (full line). The spectra for the two-hole state have a y-scale enlarged by 100 with respect to column $k_T=\pi$.

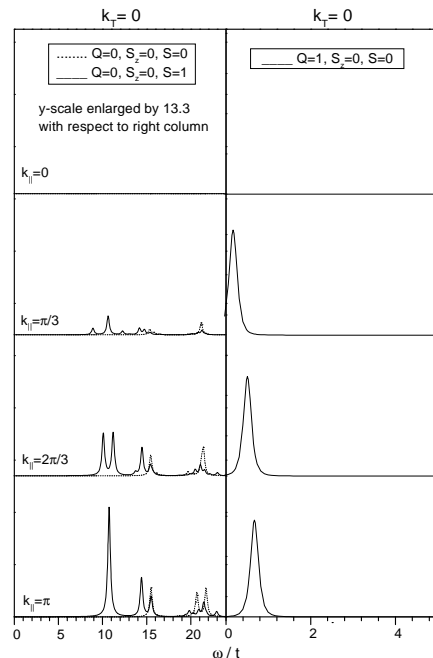


FIG. 12. Comparison of the density correlation spectrum for the half-filled ground state (dotted line, left), the ${}^3(\pi, \pi)_0$ state with $S_z=0$ (full line, left), and the two-hole ground state (right). Parameter values are as in Figure 6.

identity relationships in the present case depend very much on the representations (27) and (30) of the spin and density operators in terms of the rung Bosons. While these are easily transferable to ladder-like systems, analogous identities for a fully planar system may be quite different and more restricted.

VI. ADIABATIC CONNECTION TO THE T-J MODEL

So far, we have studied the spectra for the ideal $SO(5)$ symmetric model. In this section we want to investigate the effect of discarding the correction terms H_1 which enforced exact $SO(5)$ symmetry. More precisely our goal is to find, in the spirit of Landau's Fermi liquid theory, a 'mapping' between the excitation spectrum of the exactly $SO(5)$ symmetric but in principle unphysical model, and that of a 'physical' $t-J$ ladder. The latter, being the $U \rightarrow \infty$ limit of the Hubbard model, incorporates the constraint of no double occupancy which, based on erroneous mean-field calculations, has recently been argued to break $SO(5)$ symmetry [25]. We compare the single particle spectra as well as the spin correlation (i.e. a two particle spectrum) of the $SO(5)$ symmetric ladder and the $t-J$ model for a 6-rung ladder. Thereby we adjust the parameters of the $SO(5)$ symmetric ladder so as to obtain an optimal fit to the $t-J$ model, for which we fix $t_{\perp}/t=0.5$ and $J/t=0.5$, $J_{\perp}/t=2.0$. We are using a relatively large value of the exchange along the rungs, J_{\perp} - this is by no means adequate to describe actual materials, but our main goal here is to investigate the effect of the constraint of no double occupancies in the $t-J$ model. Note that the $t-J$ model has a 'Hubbard gap' which is effectively infinite, whereas in the $SO(5)$ symmetric ladder hole-doped to electron-doped states are degenerate. The models thus appear at first sight entirely unrelated, but our goal is to check our above conjecture that as long as we restrict ourselves to the hole doped sector, the two models still can well have essentially the same low-energy dynamics.

Figure 13 and Figure 14 show the photoemission spectra originating from the half-filled ground state $^1(0,0)_0$, and $^3(\pi,\pi)_0$ with $S_z=0$. The overall agreement of the two model's spectra was obtained choosing $U/t=4$, $V/t=-3.25$, $J/t=3$, and $t_{\perp}/t=2/3$ for the exactly $SO(5)$ symmetric model, followed by an energy rescaling by a factor of 0.625 (which amounts to setting $t_{SO(5)}=0.625t_{t-J}$). The resulting mapping is excellent: the $t-J$ model's number of peaks, their weight distribution and dispersion are accurately obtained also in the exactly $SO(5)$ symmetric model. In particular, the appearance of the 'sidebands' in the spectra for spin polarized ground states can be nicely seen for both models. Regarding the spin correlation for the same set of parameters (Figure 15), there is still good agreement as to

the

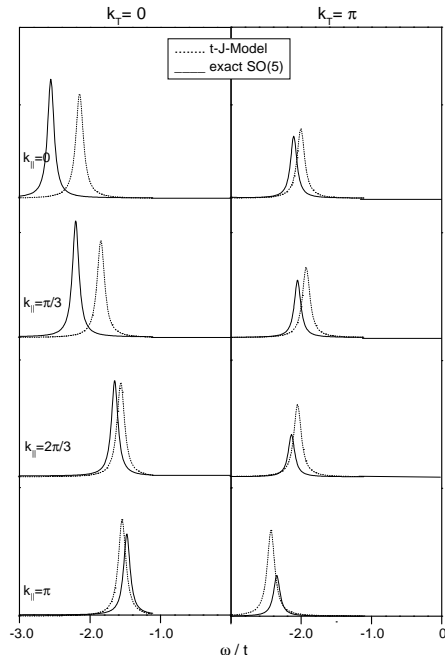


FIG. 13. Comparison of the photoemission spectra from the half-filled ground state of the $t-J$ model (dotted line) and the exact $SO(5)$ model (full line). The $t-J$ parameters are $t_{\perp}/t=0.5$, $J/t=0.5$, $J_{\perp}/t=2$, the $SO(5)$ parameters $t_{\perp}/t=2/3$, $U/t=4$, $V/t=3.25$, $J/t=3$, with $t_{SO(5)}=0.625t_{t-J}$.

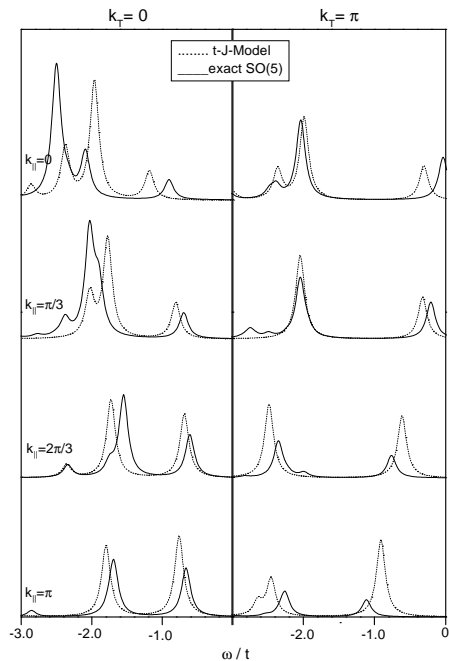


FIG. 14. Comparison of the photoemission spectra from the half-filled $^3(\pi,\pi)$ state with $S_z=0$ of the $t-J$ model (dotted line) and the exact $SO(5)$ model (full line). Parameters are as in Figure 13.

number and the weight of the peaks and the character of the dispersion. The absolute size of the dispersion is somewhat smaller in the exact $SO(5)$ model but the value of the ‘spin gap’ at (π, π) is reproduced quite accurately. Altogether, the mapping between the ‘unphysical’ but exactly $SO(5)$ symmetric model and the physically better founded $t-J$ model is reasonably good, which clearly supports the physical relevance of $SO(5)$ symmetry. We also note that the calculations are ‘as close as possible’ to half-filling, where the impact of the Hilbert-space projection still is presumably the largest in the $t-J$ model - yet the agreement of the low-energy physics is obviously quite good. One therefore may hope that similar mappings can be carried out also for more realistic parameter values of $t-J$ ladders, so that for $t-J$ and Hubbard ladders the $SO(5)$ symmetric model may in fact be the generic effective Hamiltonian. This is further supported by numerical studies in the case of large $U=-V$, $J=0$ [27] recently carried out by Duffy, Haas and Kim, and renormalization group calculations [16,17] for the weak coupling case.

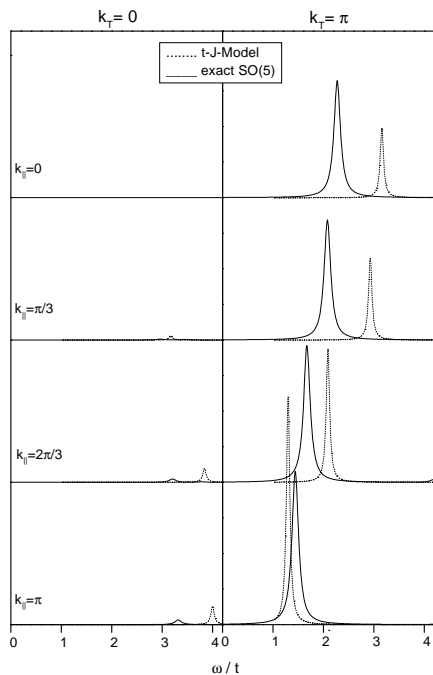


FIG. 15. Comparison of the spin correlation spectra for the half-filled ground state of the $t-J$ model (dotted line) and the exact $SO(5)$ model (full line). Parameters are as in Figure 13.

VII. CONCLUSION

In summary, we have studied the dynamics of an exactly $SO(5)$ symmetric ladder model. We have shown that in the strong-coupling limit the model reduces to

the simplest possible $SO(5)$ symmetric generalization of a Bosonic Model derived previously by Gopalan *et al.* [18] for the spin excitations of Heisenberg ladders. In this limit the ‘vacuum’ of the theory is the rung-RVB state, and the elementary excitations of the $SO(5)$ symmetric ladder correspond to uncharged triplet-like and charged singlet-like Bosons. $SO(5)$ symmetry then simply states that the spin-like and charge-like Bosons are dynamically equivalent, in the same sense as e.g. proton and neutron are considered dynamically equivalent in the isospin theory of nuclear physics. In the strong coupling limit, the low energy physics can be mapped onto a model of five species of hard-core bosons. The effective non-linear σ model description [1] can be systematically derived in this limit.

Because the ground state of the ladder system is a Mott insulator with ‘RVB type’ of singlet vacuum, it can serve as a reference state to consider the condensation of magnons and charged bosons on the equal footing, thereby revealing the precise analogy between antiferromagnetism and superconductivity. In a 2D system, no such reference state is found to be the ground state for any reasonable Hamiltonian in the infinite system. However, the ground state of any finite cluster is a total spin singlet, and recent numerical calculations [6,7] demonstrate that the ground state of the $t-J$ or Hubbard model is also approximately a $SO(5)$ singlet. The low energy excitations of the 2D cluster are magnons and hole pairs, and share many similarities to the properties of the $SO(5)$ ladder system found in this work.

As shown in the present work, $SO(5)$ symmetry has profound implications for the dynamical correlation functions, most notably the single particle spectrum. Specific predictions of $SO(5)$, like a ‘generalized rigid band behaviour’ [2,5] and the appearance of sidebands in the inverse photoemission spectrum [24] may indeed have been observed long ago in the actual 2D $t-J$ model. Motivated by the present theory we have carried out more detailed spectroscopies on the 2D model and obtained results in strong support of $SO(5)$ [26].

Finally we (and other authors [16,17,27]) have demonstrated that despite the at first sight rather unphysical parameter values of the $SO(5)$ symmetric model, a ‘Landau mapping’ to the more realistic $t-J$ model is feasible. This may suggest that the $SO(5)$ symmetric ladder is in fact the generic effective Hamiltonian for two-leg ladder systems.

Acknowledgements: Two authors (W.H. and S.C.Z.) have benefitted from many enlightening discussions with D. J. Scalapino. SCZ is supported in part by the NSF under grant numbers DMR94-00372 and DMR95-22915. A.D., M.G.Z. and W.H. acknowledge support from DFN contract TK598-VA/D3 and are grateful to the University of Stuttgart and München Supercomputing Centers. R. E. most gratefully acknowledges the kind hospitality at the National Center for Theoretical Studies, National Tsing

VIII. APPENDIX

We consider the coherent state

$$|\Psi_\lambda\rangle = \frac{1}{\sqrt{n}} e^{\lambda\sqrt{N}t_z(\pi)^\dagger} |vac\rangle,$$

where n is the normalization factor, and $t_z(\pi)^\dagger$ the creation operator for a true *hard-core* Boson. Let us assume that the exponential has been expanded, and ask for the total norm, n_ν , of all states of ν^{th} order in λ (i.e. all states containing ν Bosons). Each of these terms has a prefactor of $\lambda^\nu/\nu!$ from the expansion of the exponential. There is also a factor of ± 1 , depending on how many Bosons are on rungs with odd numbers - this will disappear upon squaring the prefactor and we therefore disregard it. Moreover, the factor of $1/\nu!$ is cancelled because each Boson configuration is generated in $\nu!$ different ways when expanding $(t_z(\pi)^\dagger)^\nu$. The number of different Boson configurations (which are mutually orthogonal!) with ν Bosons is $N!/(N-\nu)!$, whence

$$n_\nu = \lambda^{2\nu} \binom{N}{\nu},$$

and summing over ν we obtain

$$n = (1 + \lambda^2)^N.$$

Next, we have

$$\sqrt{N}t_z(\pi)^\dagger|\Psi_\lambda\rangle = \partial_\lambda(\sqrt{n}|\Psi_\lambda\rangle),$$

whence

$$\begin{aligned} \langle\Psi_\lambda|M_S|\Psi_\lambda\rangle &= \frac{1}{\sqrt{2}}\partial_\lambda \log(n) \\ &= \frac{\sqrt{2}\lambda N}{1 + \lambda^2}, \end{aligned}$$

q.e.d.

[1] S.C. Zhang, *Science* 275, 1089 (1997).

[2] R. Eder, Y. Ohta, and S. Shimozato, *Phys. Rev. B* **50**, 3350 (1994).

- [3] R. Eder, Y. Ohta, and S. Maekawa, *Phys. Rev. Lett.* **74**, 5124 (1995).
- [4] R. Preuss, W. Hanke, W. von der Linden, *Phys. Rev. Lett.* **75**, 1344 (1995).
- [5] S. Nishimoto, Y. Ohta, and R. Eder, *Phys. Rev. B* **57**, 14247 (1997).
- [6] S. Meixner, W. Hanke, E. Demler, and S. C. Zhang, *Phys. Rev. Lett.* **79**, 4902 (1997).
- [7] R. Eder, W. Hanke, and S. C. Zhang, *cond-mat/9707233*.
- [8] E. Demler, and S. C. Zhang, *Phys. Rev. Lett.* **75**, 4126 (1995).
- [9] Z. Hiroi, M. Azuma, M. Takano, and Y. Bando, *J. Solid State Chem.* **95**, 230, (1991).
- [10] M. Azuma, Z. Hiroi, M. Takano, K. Ishida, and Y. Kitaoka, *Phys. Rev. Lett.* **73**, 3463 (1994).
- [11] M. Uehara, T. Nagata, J. Akimitsu, H. Takahashi, N. Mori, and K. Kinoshita, *J. Phys. Soc. Jpn.* **65**, 2764 (1996).
- [12] E. Dagotto and T. M. Rice, *Science* **271**, 618 (1996).
- [13] J. M. Tranquada, B. J. Sternlieb, J. D. Axe, Y. Nakamura, and S. Uchida, *Nature* **375**, 661 (1995).
- [14] D. Poilblanc and T. M. Rice, *Phys. Rev. B* **39**, 9749 (1989); J. Zaanen and O. Gunnarson, *Phys. Rev. B* **40**, 7391 (1989); H. Eskes, R. Grimberg, W. van Sarloos, and J. Zaanen, *Phys. Rev. B* **54**, R724 (1996); V. Emery, S. Kivelson and O. Zacher, *Phys. Rev. B* **56**, 6120 (1997).
- [15] D. J. Scalapino, S. C. Zhang, and W. Hanke, *Phys. Rev. B*, accepted for publication.
- [16] E. Arrigoni and W. Hanke, *cond-mat/9712143*.
- [17] H. H. Lin, L. Balents, and M. P. A. Fisher, *cond-mat/9801285*.
- [18] S. Gopalan, T. M. Rice, and M. Sigrist, *Phys. Rev. B* **49**, 8901 (1994).
- [19] R. Eder, *cond-mat/9712003*.
- [20] T. Barnes, E. Dagotto, J. Riera, and E. S. Swanson, *Phys. Rev. B* **47**, 3196 (1993); H. Endres, R. M. Noack, W. Hanke, D. Poilblanc, and D. J. Scalapino, *Phys. Rev. B* **53**, 5530 (1996); G. Sierra and M. A. Martin-Delgado, *Phys. Rev. B* **56**, 8774 (1996); E. Dagotto, G. B. Martins, J. Piekarewicz, and J. R. Shepard, *cond-mat/9707205*; I. Bose and S. Gayen, *Phys. Rev. B* **48**, 10653 (1993); H. Tsunetsugu, M. Troyer, and T. M. Rice, *Phys. Rev. B* **49**, 16078 (1994); M. Troyer, H. Tsunetsugu, and T. M. Rice, *Phys. Rev. B* **53**, 251 (1996). B. Frischmuth, B. Ammon, and M. Troyer, *Phys. Rev. B* **54**, 3714 (1996).
- [21] S. Sachdev and R. N. Bhatt, *Phys. Rev. B* **41** 9323 (1990).
- [22] J. P. Hu and Shou-Cheng Zhang, "Review of $SO(5)$ Group Theory", to be published.
- [23] E. Dagotto, *Rev. Mod. Phys.* **67**, 63 (1994).
- [24] R. Eder, Y. Ohta, *Phys. Rev. B* **54**, 3576 (1996).
- [25] M. Greiter, *Phys. Rev. Lett.* **79**, 4898 (1997).
- [26] R. Eder *et al.* to be published.
- [27] D. Duffy, S. Haas, and E. Kim, *cond-mat/9804221*.